The role of the viscous sublayer in calcium carbonate dissolution

Christopher M. Fellows[a,b,*], Ali A. Al-Hamzah[a,b], Gaheishi A.H. Al-Dowis[a],
Michael G. Evans[b], Mohammed Mahmoodur Rahman[a]

[a]*Desalination Technologies Research Institute, Saline Water Conversion Corporation, Al-Jubail 31951, Kingdom of Saudi Arabia,
Tel. +966 13 3430333; Ext. 31703; emails: cmichael@swcc.gov.sa/cfellows@une.edu.au (C.M. Fellows), aal-hamzah2@swcc.gov.sa
(A.A. Al-Hamzah), galdowis@swcc.gov.sa (G.A.H. Al-Dowis), mrahman4@swcc.gov.sa (M.M.Rahman)*
[b]*School of Science and Technology, The University of New England, NSW 2351, Australia, email: mevans2@une.edu.au (M.G. Evans)*

ABSTRACT

Remineralization is a key component of post-treatment of desalinated water, particularly that obtained by thermal desalination, to avoid corrosion in distribution systems and address human health concerns. Dissolution of limestone under an elevated pressure of carbon dioxide is a common remineralization procedure. Prompted by the desire to optimize this process, we examined literature data on its kinetics and found that there was no consensus on the mechanism of dissolution or the nature of the rate-controlling step. We propose a steady-state model, where there is a locally constant concentration of solute in a surface layer of solvent, with the rate of dissolution controlled by transport into and out of this surface layer. This model can explain the wide variation reported in experimental rate coefficients for calcium carbonate dissolution and fit experimental data obtained under very different systems with physically reasonable values for the dimensions of the viscous sublayer.

Keywords: Remineralization; Post-treatment; Kinetics; Calcium carbonate

1. Introduction

Dissolution of solids in liquids is a phenomenon familiar to everyone from their daily lives. To all appearances, it would seem to be a simple one, and considering how critical it is to many industrial processes of enormous importance, it would be reasonable to expect that it had been well-understood by this time. However, this does not seem to be the case [1], despite impressive advances in the methods available for its study [2]. The kinetics of dissolution is frequently expressed in empirical terms without a clear mechanistic significance [3,4], and rate equations are often expressed as functions of the extent of reaction, $1 - \Omega$ (where $\Omega = Q_{sp}/K_{sp}$), a measure of the thermodynamic favorability of the process that has no in-principle connection to its kinetics (Fig. 1) [5,6].

This paper will discuss one particular case of dissolution, that of calcium carbonate. This is of significance geologically, as a major factor in the evolution of karst landscapes [11], and socio-politically, as a constraint on the impact of the postulated "de-alkalinization" of oceanic surface waters [12], and in desalination, as the key reaction in many remineralization systems [13]. There is no clear consensus on the appropriate rate expression for dissolution of calcium carbonate [14] which reflects an unclear picture of the underlying mechanisms. At present processes for remineralization of desalinated water by calcium carbonate dissolution with carbon dioxide typically require amounts of carbon dioxide in excess of the stoichiometric amount which must be removed by degassing or neutralization with base after remineralization [15,16], and a clearer understanding of the mechanism and kinetics should allow better management of this process by optimizing conditions for the rapid reaction of carbon dioxide and limestone.

* Corresponding author.
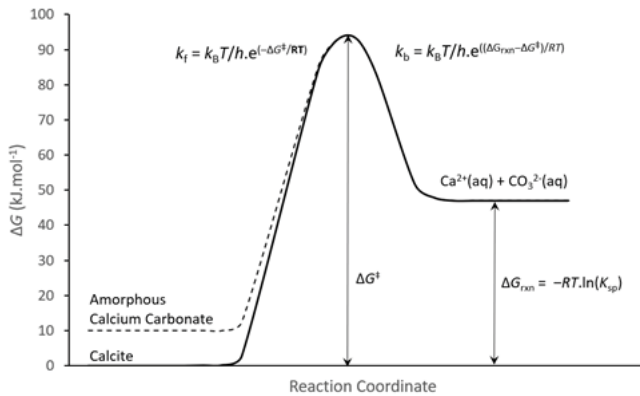
Fig. 1. Standard free energy changes in calcium carbonate dissolution.*

A model for calcium carbonate dissolution must fit experimental kinetic results obtained under a wide variety of conditions. In these studies, it has been observed that the rates of calcium carbonate dissolution:

- Fit a dependence on $(1 - \Omega^{1/2})$, where $\Omega = [Ca^{2+}][CO_3^{2-}]/K_{sp}$ [17–19],
- At high $[CO_2]$, fit a straight line with $[CO_2]$, but with an appreciable y-intercept at $CO_2 = 0$ (e.g., [20]),

There are strong hydrodynamic effects in the rates of dissolution, and considerable effort has been expended to remove the impact of these in many experimental studies. This is an understandable effort toward a laudable goal, but it raises two questions. Firstly, is it experimentally possible to remove all hydrodynamic effects and confirm that they are absent? The attainment of a plateau where additional increases in agitation do not provide greater dissolution is often taken as evidence that the process is no longer transport controlled, but as Bircumshaw and Riddiford [21] pointed out a long lifetime ago, this criterion must be applied with extreme care. "For some systems, it is observed that as the rate of stirring is increased the observed velocity constant reaches a limiting value, and thereafter is independent of the fluid velocity. This may be due to a change to chemical control, or to the stirrer's having reached maximum efficiency; for any given case, other criteria must be applied to distinguish between these possibilities." Secondly, given the conditions under which most natural and industrial dissolutions are carried out, to what extent will the purely chemical kinetic parameters obtained by the removal of all

_____

*Approximate Gibbs free energy difference between calcite and amorphous calcium carbonate and ions in solution are obtained from K_{sp} values [7,8]. While the Eyring-Polanyi model strictly holds only for a model with a single elementary step [9,10], which this is not, $\Delta G^{\ddagger}$ has been approximated from the range of E_A values quoted by Petrou and Terzidaki for the dissolution reaction [6] and an *a priori* estimate for $\Delta S^{\ddagger}$: since the reaction as drawn is strongly endothermic, the transition state should resemble the products, that is, hydrated ions imposing a great deal of order on the solution, and thus $\Delta S^{\ddagger} - \Delta S_{rxn}$, which is about -200 J K^{-1} mol^{-1}. Using $\Delta G^{\ddagger} = E_A - RT - T \cdot \Delta S^{\ddagger}$ gives $\Delta G^{\ddagger}$ between 72 and 116 kJ mol^{-1} for the forward reaction for calcite, implying $\Delta G^{\ddagger}$ between 25 and 69 kJ mol^{-1} for the backward reaction.

hydrodynamic effects be of significant use in understanding these processes? That is, can a model that excludes hydrodynamic effects be easily extended for application to systems of practical interest?

The approach of this document will be to incorporate both physical and chemical events in the one model, rather than attempt to remove physical effects and isolate chemical ones. This is the approach that has been followed to good effect, *inter alia*, in the study of the kinetics of emulsion polymerization [22,23].

2. Results

2.1. General kinetics of dissolution

The most general starting equation for dissolution considers an equilibrium where the net dissolution rate is obtained from the rates of forward and backward reactions.

$$R_{diss} = R_f - R_b \tag{1}$$

where,

$$R_b = k_b \gamma_{Ca} \gamma_{CO_3} [Ca^{2+}][CO_3^{2-}] \tag{2}$$

where k_b is the rate coefficient of the backward reaction and γ_{Ca} and γ_{CO_3} are the activity coefficients of Ca^{2+} and CO_3^{2-}. The initial formation of aquated ions, $Ca^{2+}(aq)$ or $CO_3^{2-}(aq)$, from $CaCO_3(s)$ from an area of surface with rate R_f will lead to an increase in the concentration of $Ca^{2+}(aq)$ and $CO_3^{2-}(aq)$ in the immediate vicinity of the dissolving surface. If these are not transported away, the rate of the backward reaction, R_b will invariably increase until $R_f = R_b$ and the net reaction ceases.

Transport away from the surface can be best modeled as a process driven by the concentration gradient $\Delta c/\Delta x$ [24]:

$$R_t = E\left(\frac{\Delta c}{\Delta x}\right) \tag{3}$$

In general, E will be an "eddy diffusion coefficient" of magnitude of order 10^{-6}–10^{-7} m^2 s^{-1}. These coefficients scale as $\varepsilon^{1/3} d_{max}^{4/3}$ [25], where ε (W kg^{-1}) is the energy dissipation rate and d_{max} (m) is the characteristic maximum size of the eddies in the system, so it is unlikely that E values much greater than 10^{-4} m^2 s^{-1} can be achieved under the most energetic agitation.

In systems, such as seawater where $[Ca^{2+}]$ is everywhere high relative to $[CO_3^{2-}]$, this transport rate would become:

$$R_t = E\left(\frac{\Delta\left[CO_3^{2-}\right]}{\Delta x}\right) \tag{4}$$

but in general, it can be expected to depend on the total concentration,

$$R_t = E\left(\frac{\left(\Delta\left[CO_3^{2-}\right] + \Delta\left[Ca^{2+}\right]\right)}{\Delta x}\right) \tag{5}$$

In stagnant waters, and for some distance from the surface under moderately energetic conditions of agitation where the flow is laminar, transport will be by molecular diffusion, and E will become the "molecular diffusion coefficient" D of the magnitude of order 10^{-9} m^{2}s^{-1} [26]. Most importantly, even under highly energetic conditions where

there is turbulent flow, the liquid directly in contact with the surface will comprise a viscous sublayer in which flow is laminar and there will be no net transport of solute away from the dissolving surface. The thickness of this sublayer may be from 1% to 20% of the thickness of the turbulent boundary layer [27]. Note, however, that this is not a static layer. There are likely to be transient dynamic regions dependent on surface morphology where turbulent flow impacts directly on the surface [28].

Thus, when considering the generalized dissolution of $CaCO_3$ in terms of the change in concentration of the dissolved ions $[Ca^{2+}]$ and $[CO_3^{2-}]$ (Fig. 2) there are three processes which may be rate determining:

(i) The chemical process, $R_f - R_b$
(ii) Transport through the zone of molecular diffusion, R_t (D)
(iii) Transport through the zone of eddy diffusion, R_t (E)

It is evident experimentally that agitation can accelerate dissolution at all values of Ω, so step (iii) must be rate determining, at least at low levels of agitation. However, in

retarding the overall rate of the reaction, step (iii) will necessarily increase R_b until a steady state is reached such that $R_t = R_f - R_b$; if this was not the case, the concentration of Ca^{2+} and CO_3^- at the high concentration end of the zone would rise indefinitely. Can the level of agitation be increased so that step (i) is rate-determining such that:

$$R_{diss} = R_f - k_b \, \gamma_{Ca} \gamma_{CO_3} \, [Ca^{2+}]_{bulk}[CO_3^{2-}]_{bulk} \qquad (6)$$

(The expression that is the starting point for most derivations of dissolution kinetics)? In principle, it would appear so, as this will be the lowest possible limit of R_b, solution removed at such a value of R_t will only be replaced by the material of the same composition, leaving R_b unchanged. Thus, Eq. (6) will define an envelope of the maximum possible rate at any $[Ca^{2+}]_{bulk}$ and $[CO_3^{2-}]_{bulk}$. Transport limitations will lead to curves below this one.

If R_f were given by $c.k_f$ for all values of Ω, where c was a constant, and if k_f itself was constant as a function of Ω, the commonly used expression which is often traced back to the work of Aagaard and Helgeson [29] on silica dissolution, $R_{diss} = k \, (1 - \Omega)$, would clearly follow from the dependence of the difference between k_f and k_b on ΔG_{rxn}. Note first that rates are defined here in terms of concentration change per unit of surface area so that if the specific surface area does not vary significantly with Ω, c should be constant. However, it is likely that more reactive asperities will be removed more readily further from saturation, giving a reduction in specific surface area with time [30,31]. More importantly, it is abundantly clear that calcium carbonate surfaces evolve over time and exchange material with the solution in a way that implies that k_f will depend on Ω. Note first the copious literature on atomic force microscopy experiments showing dissolution predominantly at high energy sites (kinks and edges) whose distribution varies with time [32–34]. These high energy sites will be at different positions on the left-hand side of Fig. 1, elevated with respect to the thermodynamic value applicable at saturation which is used to determine k_f. Note also that saturation, the surface will necessarily be covered with a labile layer of the most readily formed polymorph of calcium carbonate, amorphous calcium carbonate (ACC), which at some stage as R_b falls must be replaced by a surface of calcite (or aragonite or vaterite, depending on what polymorph is being dissolved). Thus as Ω is reduced from 1 toward 0, one would expect a number of changes in R_f. (1) A decrease due to replacement of ACC with the underlying substrate mineral. (2) A decrease due to smoothing with the removal of asperities. (3) an increase as etching phenomena lead to greater densities of edge and kink sites.

Finally, there is no reason for $\Delta G^{\ddagger}$ to remain constant with Ω. The transition state should be similar to the structure of the product, but increasing concentrations of ions on the product side will change the nature of the solvation in the transition state, probably giving a larger enthalpic and reduced entropic contribution.

The relative magnitudes of D and E suggest that under low energy conditions (e.g., in quiescent waters), (ii) will normally be slower than, (iii) and can be assumed to be the rate-controlling step of the process. Under high energy conditions where the dimensions of the laminar layer where D applies are reduced, it is clear that, (iii) will be
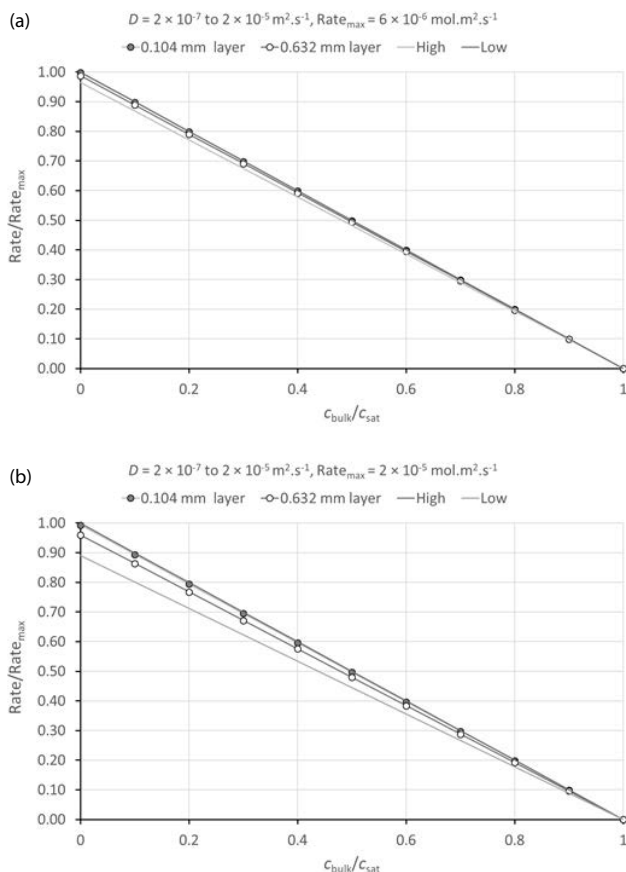
Fig. 2. Impact of transport through a turbulent boundary layer on dissolution rates of $CaCO_3$ for (a) R_{max} = 6 × 10⁻⁶ mol m² s⁻¹ and (b) R_{max} = 2 × 10⁻⁵ m² s⁻¹. The 0.104 and 0.632 mm values are calculated for turbulent boundary layers of those thicknesses with D = 1 × 10⁻⁶ m² s⁻¹. "High" and "Low" refer to the combination of the extreme values of D with the extreme values of the thickness of the turbulent boundary layer expected in the rotating disk experiments reported by Colombani [17].

the rate-controlling step of the process. As the rate of (iii) is increased further so that it is no longer rate-controlling, will (ii) or (i) become the rate-controlling step of the dissolution? Work in this field to date has assumed that at high agitation rates, there is no laminar layer (ii), so this question does not arise, but as noted above a turbulent boundary layer will incorporate a viscous sublayer where transport will be dependent on molecular diffusion.

2.2. Dissolution of a molecular solute

Before considering the case of calcium carbonate, we will consider a molecular solute where the complexities introduced by an ionic solute (i.e., the presence of a sum of concentrations in the diffusion expression and a product of activities in the precipitation expression) are absent.

At saturation:

$$R_f = R_b = k_b \cdot \gamma \cdot c_{sat} \tag{7}$$

If we assume the transition state is the same under all saturation conditions, which is appropriate for low values of c_{sat}, then the same R_f and k_b should apply, allowing the approximation.

$$R_{diss} = k_b \cdot \gamma \cdot c_{sat} - k_b \cdot \gamma \cdot c_{surf} \tag{8}$$

where c_{surf} is the effective concentration of the dissolving species in surface layer. At the same time, the rate of diffusion will be given by:

$$R_{diff} = \frac{D(c_{surf} - c_{bulk})}{\Delta x} \tag{9}$$

where Δx is the shortest straight line distance between the volume where $c_x = c_{surf}$ and the volume where $c_x = c_{bulk}$.

Under steady-state conditions:

$$R_{diss} = R_{diff} \tag{10a}$$

$$k_b \cdot \gamma \cdot c_{sat} - k_b \cdot \gamma \cdot c_{surf} = \frac{D(c_{surf} - c_{bulk})}{\Delta x} \tag{10b}$$

$$\Delta x \cdot k_b \cdot \gamma \cdot c_{sat} - \Delta x \cdot k_b \cdot \gamma \cdot c_{surf} = D(c_{surf} - c_{bulk}) \tag{10c}$$

$$\Delta x \cdot k_b \cdot \gamma \cdot c_{sat} + D \cdot c_{bulk} = D \cdot c_{surf} + \Delta x \cdot k_b \cdot \gamma \cdot c_{surf} \tag{10d}$$

$$c_{surf} = \frac{(\Delta x \cdot k_b \cdot \gamma \cdot c_{sat} + D \cdot c_{bulk})}{(D + \Delta x \cdot k_b \cdot \gamma)} \tag{11a}$$

This is the same expression found by Colombani [35]. Where D is small, c_{surf} will clearly go to c_{sat}. Note that in applying this expression to attempt to remove hydrodynamic effects from experimental data, it would be appropriate first to use whatever eddy diffusion coefficient can be estimated in the system, rather than the molecular diffusion coefficient, that is,

$$c_{surf} = \frac{(\Delta x \cdot k_b \cdot \gamma \cdot c_{sat} + E \cdot c_{bulk})}{(E + \Delta x \cdot k_b \cdot \gamma)} \tag{11b}$$

An expression for R_t including both hydrodynamic and chemical contributions can be readily derived. Taking again the condition that in the steady-state $R_{diss} = R_{diff} = R_t$:

$$R_{diss} = \frac{k_b \cdot \gamma \cdot c_{sat} - k_b \cdot \gamma \cdot (\Delta x \cdot k_b \cdot \gamma \cdot c_{sat} + D \cdot c_{bulk})}{(D + \Delta x \cdot k_b \cdot \gamma)} \tag{12a}$$

$$R_{diss} = \frac{k_b \cdot \gamma \cdot c_{sat} - k_b \cdot \gamma \cdot c_{sat}(\Delta x \cdot k_b \cdot \gamma \cdot c_{sat} + D \cdot c_{bulk})}{(D \cdot c_{sat} + \Delta x \cdot k_b \cdot \gamma \cdot c_{sat})} \tag{12b}$$

Defining $k = k_b \cdot \gamma \cdot c_{sat}$ gives:

$$R_t = k \left(\frac{1 - (\Delta x \cdot k + D \cdot c_{bulk})}{(\Delta x \cdot k + D \cdot c_{sat})} \right) \tag{13}$$

Clearly the term $(1 - (\Delta x \cdot k + D \cdot c_{bulk})/(\Delta x \cdot k + D \cdot c_{sat}))$ will go to $(1 - \Omega)$ as $\Delta x \cdot k$ goes to 0, that is,

$$R_t \rightarrow k(1 - \Omega) \tag{14}$$

As $\Omega = c_{bulk}/c_{sat}$ for a molecular solute.

The boundary layer as defined in hydrodynamics, δ, is a quantity defining the distance from a surface where the velocity of the fluid is retarded relative to the bulk velocity. For purposes of estimating whether diffusion steps are rate-limiting, δ can be equated to Δx, although it is possible to postulate a steeper concentration gradient, mass balance means that the concentration of a solute in a volume moving more slowly than the bulk cannot remain the same as the bulk concentration. Estimation of the thickness of the boundary layer requires an estimate of the eddy diffusion coefficient. Dreybrodt used the expression $E = 10^4 \times D$ [36], which would give $E = 10^{-5}$ m^2 s^{-1}, but this expression has no physical justification. The expression of Batchelor [37] and Richardson [38], $E = \alpha L^{4/3}$, where L is the appropriate length scale over which particle motions are correlated and α is between 2×10^{-3} and 1×10^{-2} m$^{2/3}$ s^{-1}, gives values between $E = 1 \times 10^{-8}$ and 2×10^{-5} at the mm and dm scales.

The turbulent boundary layer expression used by Colombani for flat plates, $\delta = 2.45 \times (\mu/\rho)^{1/6}u^{-1/2}E^{1/3}l^{1/2}$ [39] where μ is the dynamic viscosity of the solvent, ρ is the density of the solvent, u is the velocity of the fluid and l is a characteristic length dimension of the particle, gives boundary layer thicknesses between 128 and 632 μm for $E = 1 \times 10^6$ m^2 s^{-1} under the range of experimental conditions quoted by Colombani. A similar range of values (104–284 μm) is obtained using the expression used by Colombani for a rotating disk, $\delta = 1.61 \times E^{1/3}(\mu/\rho)^{1/6}\omega^{1/2}$ (where ω is the angular velocity of the rotating disk) under the range of conditions for which adequate experimental details are provided.

Assuming a $c_{sat} = 0.30$ mol/m^{3*} and postulating that experiments have been able to reach conditions such that $R_t \rightarrow k$ with experimental values of 6×10^{-6} or 2×10^{-5} mol m^{-2} s^{-1} [35] (which may be confirmed by assuming microscopic irreversibility and comparing the values obtained with rates

---

Note that there have been multiple experiments suggesting that the K_{sp} for ACC determined by Brečević and Nielsen [8] at 25°C, 0.40 mol^2 m^{-6}, is too large and the true value is less than 0.09 mol^2 m^{-6} [40–44].

of calcium carbonate deposition obtained under conditions slightly above saturation [45]) curves closely approximating to R_t μ $(1 - \Omega)$ are obtained for plausible thicknesses of the turbulent boundary layer (Fig. 2). It is clear that the levels of agitation achieved experimentally should be sufficient to give $R_t - R_{tmax}$, rendering eddy diffusion non-rate determining (Fig. 2).

With turbulent boundary layers of these approximate magnitudes, what will be the impact of the viscous sublayer? As noted above, the thickness of the viscous sublayer is in the range of 1%–20% of the thickness of the turbulent boundary layer [27]. Taking a relatively conservative estimate of the thickness of these layers as 5% of the thickness of the turbulent boundary layer and retaining all other conditions identical to those shown in Fig. 2 gives the curves shown in Fig. 3. Significant retardation, $R_t < R_{tmax}$, is evident, indicating that transport through this layer may become rate-determining under the conditions of agitation applied in the experiments reviewed by Colombani (Fig. 3).

Comparing Fig. 3 with the envelope of experimental reaction rates for calcium carbonate found by Colombani [17] (Fig. 4), it is evident that one possible explanation for the spread of data observed is that the analytical treatments employed have removed the effect of eddy diffusion, but not the effect of molecular diffusion through the viscous sublayer. Colombani notes that higher rates are generally obtained for smaller particles and lower rates for larger particles. As the thickness of the viscous sublayer is governed by the frictional length scale, which is a direct function of the linear dimension of the system, larger particles should have a thicker viscous sublayer, giving lower observed dissolution rates. Other potential explanations for the spread in the data, such as variations in surface roughness or speciation, have no reason to vary systematically with particle size.

In order to explain other observed features of calcium carbonate dissolution – the dependence on $[CO_2]$ and the $\Omega^{1/2}$ dependence found by Colombani – it is necessary to extend the molecular dissolution model to the case of a 1:1 ion.

2.3. Dissolution of a 1:1 ionic solute

As a first approximation, the following relationship applies over the whole course of the reaction with a constant value of k_b (cf. Eqs. (8) and (14)).

$$R_{diss} = k_b \cdot K_{sp} - k_b \cdot Q_{surf} \tag{15}$$

where Q_{surf} is the effective ion product $\gamma_M \gamma_A [M^{n+}][A^{n-}]$ of the surface layer. This relationship will be less inaccurate far from equilibrium where there will be little net deposition of ACC on the dissolving limestone surface. These far from equilibrium conditions will be those prevailing in remineralization systems [14].

The diffusive transport rates of the components of the ionic solute will be given by:

$$R_{diffM} = \frac{D_M \left([M]_{surf} - [M]_{bulk} \right)}{\Delta x_M} \tag{16a}$$

$$R_{diffA} = \frac{D_A \left([A]_{surf} - [A]_{bulk} \right)}{\Delta x_A} \tag{16b}$$

(a)

(b)
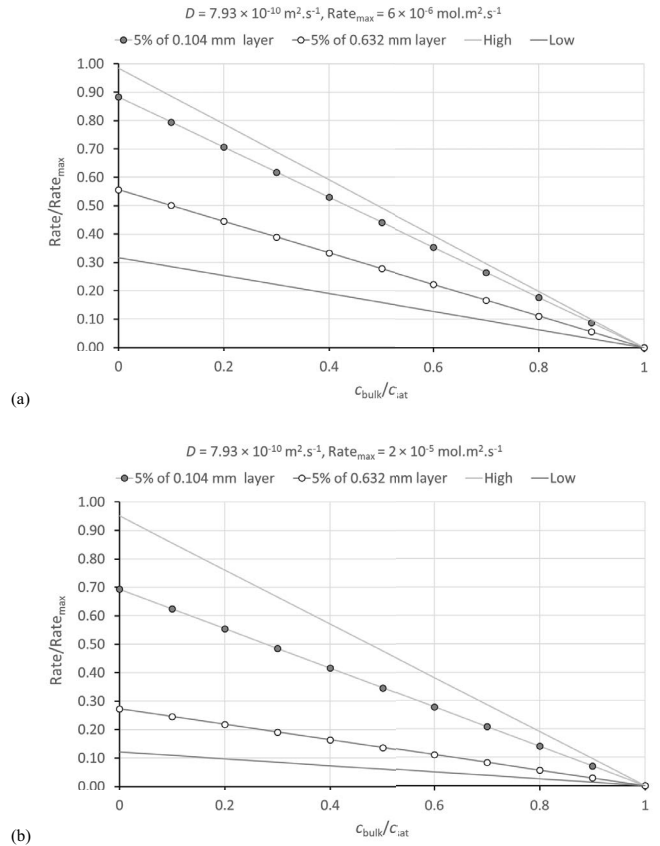
Fig. 3. Impact of diffusion through a viscous sublayer of a turbulent boundary layer on dissolution rates for (a) $R_{max} = 6 \times 10^{-6}$ mol m^2 s^{-1} and (b) $R_{max} = 2 \times 10^{-5}$ m^2 s^{-1}. "High" and "Low" refer to 5% of the extreme values of the thickness of the turbulent boundary layer expected in the rotating disk experiments reported by Colombani [17].

where $D_M = D_{Ca} = 7.93 \times 10^{-10}$ m^2 s^{-1} and $D_A = D_{CO_3} = 9.55 \times 10^{-10}$ m^2 s^{-1} [46]. To avoid charge imbalances in a system with no other ionic components, these diffusion rates should be the same. Where other ions are present, clearly their migration can balance the charge, and in seawater where the $[Ca^{2+}]_{bulk}$ is high compared to $[CO_3^{2-}]_{bulk}$ a significant counter-diffusion of Cl$^-$ can be expected. In considering the dissolution of calcium carbonate in relatively pure water, the approximation will be made that interactions between charges retard the diffusion of the faster ion and the overall rate is given by the diffusion rate of the slower species:

$$R_{diff} = \frac{D_M \left(c_{surf} - c_{bulk} \right)}{\Delta x} \tag{17}$$

where c is the concentration of all ions $= 2[M] = 2[A] = 2(Q/\gamma_M \gamma_A)^{1/2}$

Under steady state conditions such that $R_{diss} = R_{diff}$:

$$k_b \cdot K_{sp} (1 - \Omega) = \frac{D \left(c_{surf} - c_{bulk} \right)}{\Delta x} \tag{18}$$
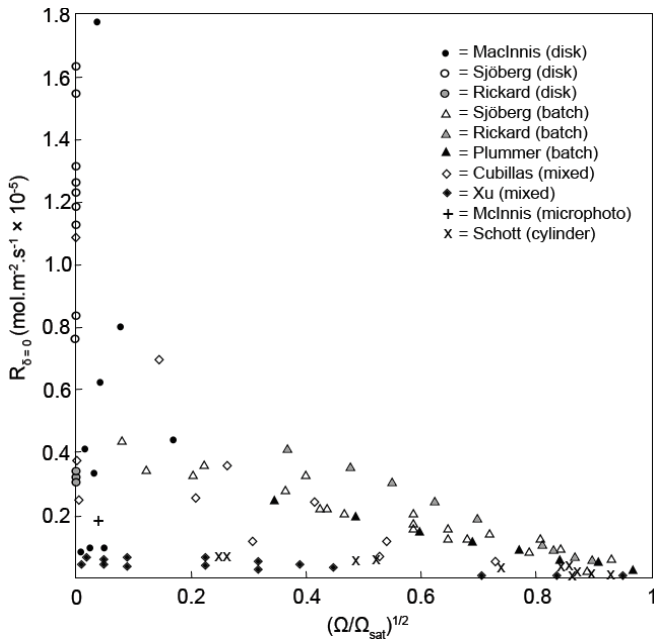
Fig. 4. Dissolution rates of calcium carbonate in similar chemical and hydrodynamical conditions (ionic strength = 0 and δ = 0) computed by Colombani, adapted from [17].

$$\Delta x \cdot k_b \cdot (K_{sp} - Q_{surf}) = D\,(c_{surf} - c_{bulk}) \tag{19}$$

An order of magnitude estimate of $(K_{sp} - Q_{surf})$ may be made given that for calcium carbonate dissolution it would appear that $k_b \cdot K_{sp} = 10^{-5} - 10^{-6}$ mol m^{-2} s^{-1}, $D = 10^{-9}$ m^2 s^{-1}, $(c_{surf} - c_{bulk}) = 10^{-1}$ mol m^{-3}, and $K_{sp} = 10^{-1}$ mol^2 m^{-6}, which implies $\Delta x\,(K_{sp} - Q_{surf}) = 10^{-5} - 10^{-6}$ mol^2 m^{-5} at low saturations. This, in turn, implies that the difference between $K_{sp} - Q_{surf}$ is only of the same order of magnitude as K_{sp} in a narrow range of Δx values, $10^{-4} - 10^{-5}$ m. Smaller values of Δx will lead to physically impossible magnitudes of this difference ($>K_{sp}$), while larger values of Δx will correspond to $K_{sp} - Q_{surf}$. This suggests that if experiments performed to date have reached the chemically-controlled rate R_f, agitated systems with Δx of order 10^{-4} m will have a zone with a $Q_{surf} > Q_{bulk}$ in this volume, similar to the general expression for dissolution proposed by Noyes and Whitney [47].

In order to obtain a full model that takes into account the effect of H$^+$ or CO$_2$ on the dissolution of calcium carbonate under distant from equilibrium conditions, we will apply another embodiment of steady-state conditions to this surface layer.

In the vicinity of a dissolving surface where laminar flow conditions apply, let us define a volume of space where the concentration can be considered to have a constant value, c_{surf}, bordered by the solid and by a volume where the concentration is increasing, c_{bulk}, with a transition zone of thickness δ' defined between them (Fig. 5). Note that we could do the same for the vicinity of a dissolving surface for which eddy diffusion conditions apply, but D would not then be well defined.

Flux into this volume will be from dissolution, with rate $R_f = k_b \cdot K_{sp}$ (ACC), and molecular diffusion inward, with rate $D \cdot c_{bulk}/\delta'$.
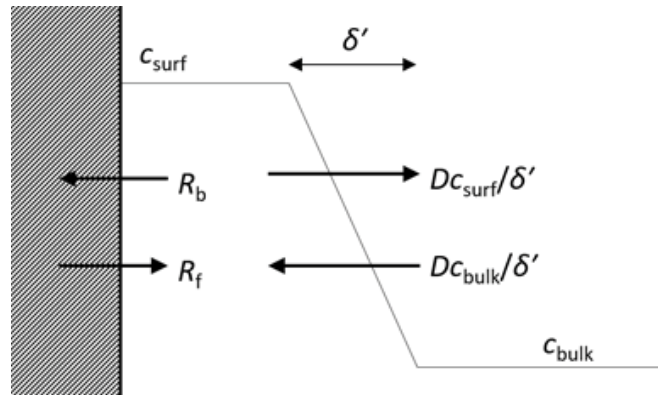
Fig. 5. Steady-state model adapted from Noyes and Whitney [47].

A constant k_b will be assumed in the first instance. While this approximation will not be accurate across all saturations for calcium carbonate, as discussed above, at low saturations the dissolving material will be calcite or aragonite, while the immediate product of precipitation will be ACC and thus $R_f = k_b.K_{sp}$ (ACC).

Flux out of this volume will be from reprecipitation, with rate $R_b = k_b \cdot Q_{surf}$, molecular diffusion outward, with rate $D \cdot c_{surf}/\delta'$, and the reaction of a reactive solute, which for a carbonate will be H$^+$ or H$_2$CO$_3$, with rate $k' \cdot \gamma_{Ca}\gamma_{CO_3} \cdot$ [CO$_2$] $\cdot$ [CO$_3^{2-}$] or $k'' \cdot \gamma_H\gamma_{CO_3} \cdot$ [H$^+$] $\cdot$ [CO$_3^{2-}$]. (Here, k' incorporates the uncertain rate coefficient for CO$_2$(aq) + H$_2$O $\rightarrow$ H$_2$CO$_3$(aq)).

In the presence of CO$_2$, it might be expected that in general there could be reactions of H$_2$CO$_3$ or H$_3$O$^+$ directly with CaCO$_3$(s), so that this process could impact the kinetics. Competition between reactions taking place on the surface and reactions taking place in the continuous phase will be important as the dimensions of the surface layer decrease with greater agitation, as the concentration of the solute decreases, and as the zeta potential of the dissolving surface becomes negative. Under remineralization conditions, relatively low agitation means that reactions are likely to be controlled by eddy diffusion, with thick surface layers, while concentrations of solute are relatively low. Estimating a surface site concentration of 6.9 µmol m^{-2} on particles of diameter 2 mm, the same amount of CO$_3^2$ would be present in a layer 24 µm thick for solution saturated with respect to ACC, a layer 210 µm thick for 0.1 c_{sat} and 1.29 mm thick for 0.01 c_{sat}. Given the likely dimension of surface layers under demineralization conditions will be greater than 1 mm, there will be considerably more carbonate available for reaction in the continuous phase than on the surface. Furthermore, the direct reaction between H$_2$CO$_3$(aq) and CaCO$_3$(s) must necessarily pass through some intermediate Ca(HCO$_3$)$_2$(s) species; this is not known to exist so this pathway must be considered to be highly thermodynamically unfavorable. Finally, any H$_2$CO$_3$ or H$_3$O$^+$ reacting directly with the surface must have avoided reacting with any other species in its diffusion toward the surface. At least under normal industrial conditions for the dissolution of calcium carbonate in solutions at moderately acidic pH [48], it would appear to be reasonable to discount the participation of surface reactions. While at very low ion strengths the zeta potential of CaCO$_3$ is negative even at low pH values [48], in seawater and even relatively low ionic

strength solutions it is positive [49]. Thus, electrostatic effects mean that direct reactions of H_3O^+ with the surface of solid $CaCO_3$ particles will be unlikely to occur in seawater.

The steady-state expression for fluxes into and out of this boundary zone will then be:

$$0 = \frac{k_b \cdot K_{sp} - k_b \cdot Q_{surf} - 4D\left(\left[Ca^{2+}\right]\left[CO_3^{2-}\right]\right)_{surf}^{1/2} - \left[Ca^{2+}\right]\left[CO_3^{2-}\right]\right)_{bulk}^{1/2}\right)}{\left(\gamma_{Ca}\gamma_{CO_3}\right)^{1/2}\delta' - k' \cdot \left[CO_2\right] \cdot \left[CO_3^{2-}\right]_{surf}} \quad (20)$$

And the rate equation:

$$Rate = \frac{k_f - k_b \cdot Q_{surf} = 4D\left(\left[Ca^{2+}\right]\left[CO_3^{2-}\right]\right)_{surf}^{1/2} - \left[Ca^{2+}\right]\cdot\left[CO_3^{2-}\right]\right)_{bulk}^{1/2}\right)}{\left(\gamma_{Ca}\gamma_{CO_3}\right)^{1/2}\delta' + k' \cdot \left[CO_2\right] \cdot \left[CO_3^{2-}\right]_{surf}} \quad (21)$$

which in the absence of CO_2 will be:

$$Rate = \frac{4D\left(\left[Ca^{2+}\right]\left[CO_3^{2-}\right]\right)_{surf}^{1/2} - \left[Ca^{2+}\right]\left[CO_3^{2-}\right]\right)_{bulk}^{1/2}\right)}{\left(\gamma_{Ca}\gamma_{CO_3}\right)^{1/2}\delta'} \quad (22)$$

Near equilibrium, $c_{surf} \rightarrow c_{sat}$, so in the absence of significant $[CO_2]$:

$$Rate \rightarrow \frac{D \cdot K_{sp}^{1/2}\left(1 - \Omega^{1/2}\right)}{\delta'} \quad (23)$$

Thus, the slope near the saturation of graphs of dissolution rate vs. $\Omega^{1/2}$ should be linear, as found by Colombani [17], and should be given by $-D.K_{sp}^{1/2}/\delta'$. Further from saturation, it is expected that $c_{surf} < c_{sat}$ and the slope of the curve should decrease, as can be seen in several of the data sets in Fig. 4.

Taking $D(Ca^{2+}) = 7.93 \times 10^{-10} \, m^2 \, s^{-1}$, $K_{sp}(ACC) = 0.10 \, mol^2 \, m^{-6}$, and the range of slopes found by Colombani (5×10^{-7} to $6 \times 10^{-6} \, mol \, m^{-2} \, s^{-1}$) gives a range of values of δ' from 42 to 500 μm.

These numbers are of approximately the same order of magnitude as values obtained by applying the expressions given in Colombani for determination of Δx with an eddy diffusion coefficient of $10^{-6} \, m^2 \, s^{-1}$ (104–284 μm for rotating disk experiments and 128–632 μm for stirred experiments for which stirring rates and indicative particle sizes were given in the supporting information) and without further tweaking of the model imply viscous sublayers of ≥10% of the thickness of the turbulent boundary layer.

Note that the diffusion term in Eq. (22) provides one plausible explanation for the observed reduction in dissolution rates in the presence of Mg [50,51], anomalous as the solubility of magnesium carbonate trihydrate is significantly greater than that of ACC [52]. If Mg is present in the surface layer in quantity sufficient that a significant amount of CO_3^{2-} is present in the form of dynamic $MgCO_3$ ion pairs [53], which form much more readily than $CaCO_3$ ion pairs [54], the effective diffusion coefficient of CO_3^{2-} would be significantly reduced.

Under conditions where the reaction of $CaCO_3$ is dominated by the reaction of dissolved carbonate with acid, $CO_3^{2-}(aq) + H_2CO_3(aq) \rightarrow 2HCO_3^-(aq)$, the steady-state model implies that:

$$Rate = \frac{D(Q_{surf}^{1/2} - Q_{bulk}^{1/2})}{\delta' + k' \cdot \delta' \cdot \left[CO_2\right] \cdot \left[CO_3^{2-}\right]_{surf}} \quad (24)$$

With the rate of carbonate removal by reaction with carbon dioxide dependent on the volume of the steady-state layer and $Q_{bulk}^{1/2}$ going to zero as the overall rate of the reaction increases. This implies that the observed rate will be a linear function of $[CO_2]$ with a positive y-intercept.

Close to saturation:

$$Rate \rightarrow \frac{D \cdot K_{sp}^{1/2}\left(1 - \Omega^{1/2}\right)}{\delta' + k'' \, \delta'\left[CO_2\right]} \quad (25)$$

where k'' will appear to be constant as $[CO_3^{2-}]_{surf}$ is relatively insensitive to Ω.

Note that the steady-state model outline above would not give a $(1 - \Omega^{1/2})$ order dependence for salts that have stoichiometries other than 1:1, but that the dependence would depend on the relationship between Q_{sp} and c_{surf}. Thus this model would imply a $(1 - \Omega)$ order dependence for silica [55], and for 1:1 salts where one of the product ions is in a large excess, which is the case for the important practical instance where $CaCO_3$ is dissolved in seawater [24]. Most importantly, note also that this dependence should also be visible in lower energy systems that are controlled by eddy diffusion, though the lack of constant values for eddy diffusion coefficients will make such data more difficult of interpretation. In demineralization systems when carbon dioxide is reacted with limestone the appropriate expression for fitting kinetic data should therefore be:

$$Rate = \frac{4E\left(\left[Ca^{2+}\right]\left[CO_3^{2-}\right]\right)_{surf}^{1/2} - \left[Ca^{2+}\right]\left[CO_3^{2-}\right]\right)_{bulk}^{1/2}\right)}{\left(\gamma_{Ca}\gamma_{CO3}\right)^{1/2}\delta' + k'' \cdot \delta'\left[CO_2\right] \cdot \left[CO_3^{2-}\right]_{surf}} \quad (26)$$

where E is the eddy diffusion coefficient for low-energy turbulent transport and δ' is of order 10^{-3} m consistent with the estimates above.

At very low pH or very high levels of agitation, direct reaction of acid on the surface is likely to become significant.

3. Comparison with experimental results

Experimental observations from the literature of calcium carbonate dissolution under conditions of relevance to remineralization are fitted to the model below.

To determine the probable thickness of the viscous sublayer around particulate calcium carbonate, the boundary layer thickness was estimated using $\delta = 0.22 \, r^{5/6}u^{5/6}$, where r is the particle radius and u is the velocity of flow, estimated from the expression of Colombani [17] for stirred systems, $u = 0.3 \, L\omega$, where L is the length of the stirrer.

3.1. Cubillas et al. [56]

In this work aragonite, calcite, and shellfish with different surface morphologies and calcium carbonate decomposition were dissolved in water at a range of final pH conditions [56].

Particle sizes of 1–1.5 mm and stirring rates of 100–700 rpm were employed, which should give turbulent transport layers of thickness between 900 μm and 1.5 mm.

While each data set had relatively few data points, they could all be plotted against the Colombani $\Omega^{1/2}$ dependence (assuming activity coefficient of 1 due to the low concentrations observed) with slopes between 1.3 and 2.1 × 10^{-6} mol m^{-2} s^{-1} (Fig. 6). Using a K_{sp} value of 0.09 mol^2 m^{-6} for ACC and D = 7.93 × 10^{-10} m^2 s^{-1}, Eq. (23) implies δ′ of between 115 and 183 μm for these systems, with δ′ always lower for the mineral samples than for the seashells. Note that these are remotely plausible values for the dimensions of a rate controlling viscous sublayer considering the likely dimensions of the boundary layer (~10% of the boundary layer thickness). Cubillas et al. [56] report a better fit to geometric surface area normalized rates than Brunauer–Emmett–Teller (BET) surface area normalized rates, which is what would be expected if the process happening at the interface was not the rate controlling one.

3.2. Peng et al. [20]

This work involved the dissolution of calcium carbonate at high temperatures under several atmospheres pressure of carbon dioxide (Fig. 7) [20]. Under these conditions, the reaction can be expected to be dominated by the [CO$_2$] term in Eq. (21), and linear plots are obtained for their data at all temperatures of rate as a function of [H$_2$CO$_3$] determined by Henry's Law.

The *y*-intercept was used to estimate an upper limit on δ′, assuming Q_{surf} = K_{sp} and that K_{sp} (ACC) scales with temperature in the same way as the scaling of K_{sp} (calcite).[7], giving values of 0.3–1.1 μm. The slopes of these curves should be given by $k' \cdot \delta' \cdot [CO_3^{2-}]_{surf}$. An Arrhenius plot of the obtained k' values assuming $[CO_3^{2-}]_{surf}$ = $[CO_3^{2-}]_{sat}$ is given in Fig. 8. It can be seen that reasonably consistent rate coefficient values are obtained over the range of experimental temperatures, with a plausible activation energy of 45 kJ mol^{-1}.
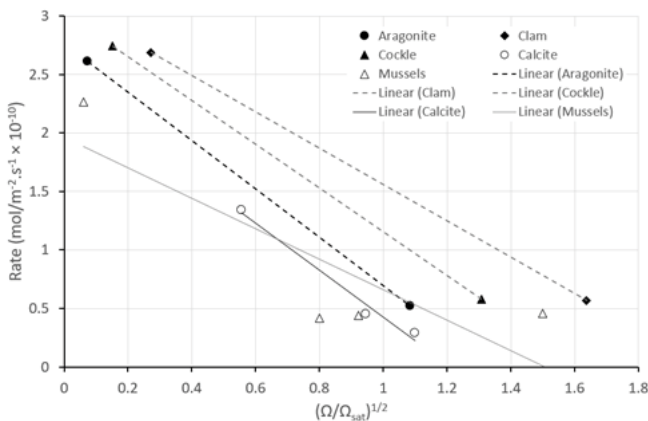
Fig. 6. Data of Cubillas et al. [56] for dissolution of calcium carbonate at 25°C at alkaline pH.
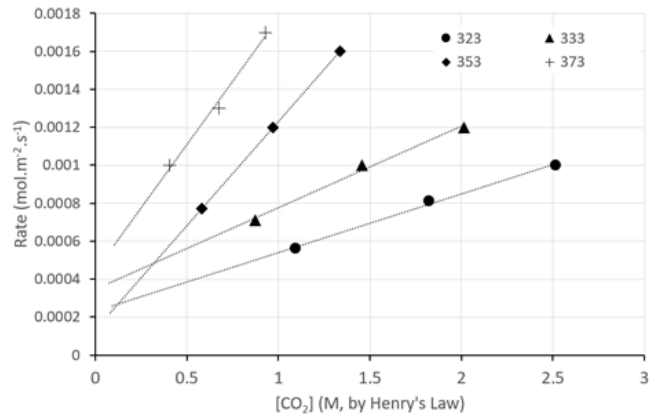
Fig. 7. Data of Peng et al. [20] for dissolution of calcium carbonate under elevated pressures of carbon dioxide at temperatures between 50°C and 100°C.
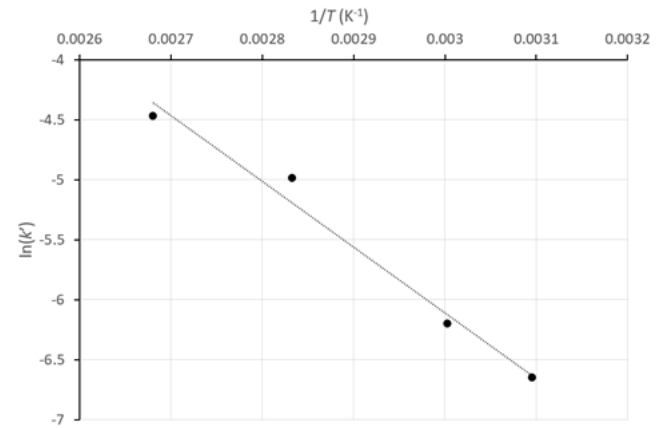
Fig. 8. Estimation of the activation energy for the reaction of H$_2$CO$_3$ and CO$_3^{2-}$ from the data of Peng et al. [20].

4. Conclusions

In this work, we have derived using the steady-state approximation for mass transfer into and out of a surface layer, a general expression for the dissolution of limestone by carbon dioxide under conditions found in limestone beds for remineralization of desalinated water:

$$\text{Rate} = \frac{4E\left(\left[\text{Ca}^{2+}\right]\left[\text{CO}_3^{2-}\right]\right)_{surf}^{1/2} - \left[\text{Ca}^{2+}\right]\left[\text{CO}_3^{2-}\right]_{bulk}^{1/2}}{\left(\gamma_{\text{Ca}}\gamma_{\text{CO}_3}\right)^{1/2}\delta' + k'' \cdot \delta'\left[\text{CO}_2\right] \cdot \left[\text{CO}_3^{2-}\right]_{surf}} \tag{27}$$

In contrast to commonly employed semi-empirical fits, every term in this model has a clear physical significance and can only be varied within relatively tight limits. We have applied this model to experimental data from the literature and have found it to be consistent with observations. The model we propose gives a unified interpretation of data on calcium carbonate dissolution obtained under various conditions relatively far from saturation and suggests hydrodynamic control of the rate of limestone dissolution under all plausible conditions within limestone/CO$_2$ demineralization systems.

Implications of this model for remineralization operations relate primarily to the optimization of particle size and flow rate. The expressions derived here for rates of dissolution in the presence of an acidic species at moderate pH include terms with both a direct and inverse dependence on the thickness of the surface boundary layer, δ. While setting conditions so that δ is as small as possible (i.e., smallest particle sizes and fastest flow rates) would be appropriate for conditions where the reaction is not controlled by reaction of dissolved carbonate ions, this will not necessarily be the case where carbon dioxide is added to provide an acidic environment. While reducing particle size will increase the surface area available for reaction, for a given velocity of flow past the particles it will also reduce the thickness of the laminar flow layer, potentially reducing the volume where carbonate ions will be present in high concentration to react with acidic species. In a similar way, increasing flow rates will reduce δ and the effectiveness of the acid treatment. Numerical modeling of the expressions derived here coupled with laboratory scale dissolution studies is proposed as a way forward to determine how close the flow rates and particle size ranges currently employed in remineralization beds approach optimum values.

Symbols

ACC	—	Amorphous calcium carbonate
BET	—	Brunauer–Emmett–Teller theory
c_{sat}	—	Saturation concentration, mol dm^{-3}
c_{surf}	—	Concentration at the solid/liquid interface, mol dm^{-3}
c_x	—	Concentration of species x, mol dm^{-3}
D	—	Molecular diffusion coefficient, m^2 s^{-1}
D_x	—	Molecular diffusion coefficient of species x, m^2 s^{-1}
d_{max}	—	Characteristic maximum eddy size, m
E	—	Eddy diffusion coefficient, m^2 s^{-1}
E_A	—	Activation energy
k	—	Rate coefficient
k'	—	Pseudo-rate coefficient for overall reaction $CO_2(aq) + CO_3^{2-}(aq) + H_2O(l) \rightarrow 2HCO_3^-(aq)$ incorporating water activity, mol^{-1} dm^3 m^{-2} s^{-1}
k''	—	Rate coefficient for overall reaction $H^+(aq) + CO_3^{2-}(aq) \rightarrow HCO_3^-$, mol^{-1} dm^3 m^{-2} s^{-1}
k_b	—	Rate coefficient for backward reaction per unit area of surface, mol^{-1} dm^3 m^{-2} s^{-1}
k_f	—	Rate coefficient for forward reaction per unit area of surface, m^{-2} s^{-1} dm^{-3}
K_{sp}	—	Solubility product
l	—	length of a dissolving particle, m
L	—	(1) Length scale over which particle motions are correlated, m; (2) length of stirrer in a stirred system, m
Q_{sp}	—	Solubility product quotient
Q_{surf}	—	Solubility product quotient at the surface
R	—	Ideal gas constant, 8.314 J K^{-1} mol^{-1}
R_b	—	Backward rate of reaction per unit area of surface, mol m^{-2} s^{-1} dm^{-3}
R_{diff}	—	Rate of diffusion per unit area of surface, mol m^{-2} s^{-1} dm^{-3}
R_{diss}	—	Rate of dissolution per unit area of surface, mol m^{-2} s^{-1} dm^{-3}
R_f	—	Forward rate of reaction per unit area of surface, mol m^{-2} s^{-1} dm^{-3}
R_t	—	Transport rate away from the surface, mol m^{-2} s^{-1} dm^{-3}
R_{tmax}	—	Maximum transport rate away from the surface, mol m^{-2} s^{-1} dm^{-3}
T	—	Temperature, K
u	—	Velocity, m s^{-1}
$[x]$	—	Concentration of species x, mol dm^{-3}
$[x]_{bulk}$	—	Bulk concentration of species x, mol dm^{-3}
$[x]_{surf}$	—	Surface concentration of species x, mol dm^{-3}
α	—	Scaling constant for estimating eddy diffusion coefficient, E, from length scale, L, m$^{2/3}$s^{-1}
γ_x	—	Activity coefficient of species x
δ	—	Boundary layer thickness, m
δ'	—	Thickness of a transition zone between two volumes of relatively constant concentration, m
Δc	—	Change in moles per unit volume, mol dm^{-3}
ΔG_{rxn}	—	Gibbs free energy of reaction, kJ mol^{-1}
$\Delta G^{\ddagger}$	—	Gibbs free energy of activation, kJ mol^{-1}
ΔS_{rxn}	—	Entropy of reaction, J K^{-1} mol^{-1}
$\Delta S^{\ddagger}$	—	Entropy of activation, J K^{-1} mol^{-1}
Δx	—	Distance over which concentration varies, m
$\Delta[x]$	—	Change in moles of species x per unit volume, mol
ε	—	Energy dissipation rate, W kg^{-1}
μ	—	Dynamic viscosity, Pa s
ρ	—	Density, kg m^{-3}
ω	—	Angular velocity, rad s^{-1}
Ω	—	Saturation, Q_{sp}/K_{sp}

References

[1] V.W. Truesdale, Evidence and potential implications of exponential tails to concentration versus time plots for the batch dissolution of calcite, Aquat. Geochem., 21 (2015) 365–396.
[2] M.D. Vinson, A. Luttge, Multiple length-scale kinetics: an integrated study of calcite dissolution rates and strontium inhibition, Am. J. Sci., 305 (2005) 119–146.
[3] R.A. Berner, J.W. Morse, Dissolution kinetics of calcium carbonate in sea water IV. Theory of calcite dissolution, Am. J. Sci., 274 (1974) 108–134.
[4] R.S. Arvidsen, I.E. Ertan, J.E. Amonette, A. Luttge, Variation in calcite dissolution rates: a fundamental problem?, Geochim. Cosmochim. Acta, 67 (2003) 1623–1634.
[5] J.W. Morse, R.S. Arvidsen, The dissolution kinetics of major sedimentary carbonate minerals, Earth Sci. Rev., 58 (2002) 51–84.
[6] A.L. Petrou, A. Terzidaki, Calcium carbonate and calcium sulfate precipitation, crystallization and dissolution: evidence for the activated steps and the mechanisms from the enthalpy and entropy of activation values, Chem. Geol., 381 (2014) 144–153.
[7] S. Alsadaie, I.M. Mujtaba, Crystallization of calcium carbonate and magnesium hydroxide in the heat exchangers of once-through multistage flash (MSF-OT) desalination process, Comput. Chem. Eng., 122 (2018) 293–305.

[8] L. Brečević, A.E. Nielsen, Solubility of amorphous calcium carbonate, J. Cryst. Growth, 98 (1989) 504–510.

[9] M.H. Evans, M. Polanyi, Some applications of the transition state method to the calculation of reaction velocities, especially in solution, Trans. Faraday. Soc., 31 (1935) 875–894.

[10] H. Eyring, The activated complex in chemical reactions, J. Chem. Phys., 3 (1935) 107–115.

[11] L. Eisenlohr, K. Meteva, F. Gabrovšek, W. Dreybrodt, The inhibiting action of intrinsic impurities in natural calcium carbonate minerals to their dissolution kinetics in aqueous H_2O-CO_2 solutions, Geochim. Cosmochim. Acta, 63 (1999) 989–1002.

[12] T. Ilyina, R.E. Zeebe, Detection and projection of carbonate dissolution in the water column and deep-sea sediments due to ocean acidification, Geophys. Res. Lett., 39 (2012), doi: 10.1029/2012GL051272.

[13] H. Shemer, D. Hasson, R. Semiat, State-of-the-art review on post-treatment technologies, Desalination, 356 (2015) 285–293.

[14] D. Hasson, O. Bendrihem, Modeling remineralization of desalinated water by limestone dissolution, Desalination, 190 (2006) 189–200.

[15] M. Hernández-Suárez, Guideline for the Remineralisation of Desalinated Waters, Canary Islands Water Center, Santa Cruz de Tenerife, 2010.

[16] G. Ozair, J.T. Gutierrez, Caustic soda injection in potabilization process, J. Sustainable Water Environ. Syst., 2 (2011) 25–36.

[17] J. Colombani, The alkaline dissolution rate of calcite, J. Phys. Chem. Lett., 122 (2016) 29285–29297.

[18] E.L. Sjöberg, A fundamental equation for calcite dissolution kinetics, Geochim. Cosmochim. Acta, 40 (1976) 441–447.

[19] E.L. Sjöberg, D. Rickard, The influence of experimental design on the rate of calcite dissolution, Geochim. Cosmochim. Acta, 47 (1983) 2281–2285.

[20] C. Peng, J.P. Crawshaw, G.C. Maitland, J.P.M. Trusler, Kinetics of calcite dissolution in CO_2-saturated water at temperatures between (323 and 373) K and pressures up to 13.8 MPa, Chem. Geol., 403 (2015) 74–85.

[21] L.L. Bircumshaw, A.C. Riddiford, Transport control in heterogeneous reactions, Q. Rev. Chem. Soc., 6 (1952) 157–185.

[22] I.A. Maxwell, B.R. Morrison, D.H. Napper, R.G. Gilbert, Entry of free radicals into latex particles in emulsion polymerisation, Macromolecules, 24 (1991)1629–1640.

[23] C.M. Fellows, R.D. Murison, G.T. Russell, Model discrimination of radical desorption kinetics in emulsion polymerisation, Macromol. Theory Simul., 20 (2011) 425–432.

[24] R.M. Pytkowicz, Chemical solution of carbonate in sea water, Am. Zool., 9 (1969) 673–679.

[25] M.N. Vlasov, M.C. Kelley, Eddy diffusion coefficients and their upper limits based on application of the similarity theory, Ann. Geophys., 33 (2015) 857–864.

[26] R.A. Robinson, C.L. Chia, The diffusion coefficient of calcium chloride in aqueous solution at 25°, J. Am. Chem. Soc., 74 (1952) 2776–2777.

[27] T. Munk, D. Kane, D.M. Yebra, The Effects of Corrosion and Fouling on the Performance of Ocean-Going Vessels: A Naval Architectural Perspective, C. Hellio, D.M. Yebra, Eds., Advances in Marine Antifouling Coatings and Technologies, Woodhead Publishing Series in Metals and Surface Engineering, Cambridge, UK, 2009, pp. 148–176.

[28] T.J. Black, Viscous Drag Reduction Examined in the Light of a New Model of Wall Turbulence, In: Proceedings of the Symposium on Viscous Drag Reduction held at the LTV Research Center, Dallas, TX, 1968, pp. 383–402.

[29] P. Aagaard, H.C. Helgeson, Thermodynamic and kinetic constraints on reaction rates among minerals and aqueous solutions, I. Theoretical considerations., Am. J. Sci., 282 (1982) 237–285.

[30] Y. Levenson, S. Emmanuel, Pore-scale heterogeneous reaction rates on a dissolving limestone surface, Geochim. Cosmochim. Acta, 119 (2013) 188–197.

[31] T.A. De Assis, F.D.A. Aarão Reis, Dissolution of minerals with rough surfaces, Geochim. Cosmochim. Acta, 228 (2018) 27–41

[32] A. Lassin, L. André, N. Devau, A. Lach, T. Beuvier, A. Gibaud, S. Gaboreau, M. Azaroual, Dynamics of calcium carbonate formation: geochemical modelling of a two-step mechanism, Geochim. Cosmochim. Acta, 240 (2018) 236–254.

[33] M. Hong, H.H. Teng, Implications of solution chemistry effects: direction specific-restraints on the step kinetics of calcite growth, Geochim. Cosmochim. Acta, 141 (2014) 228–239.

[34] K. Yuan, V. Starchenko, S.S. Lee, V. De Andrade, D. Gursoy, N.C. Sturchio, P. Fenter, Mapping three-dimensional dissolution rates of calcite microcrystals: effects of surface curvature and dissolved metal ions, ACS Earth Space Chem., 3 (2019) 833–843.

[35] J. Colombani, Pitfalls in the measurement of the true dissolution kinetics of soft minerals, Procedia Earth Planet. Sci., 7 (2013) 179–182.

[36] W. Dreybrodt, J. Lauckner, Z. Lui, U. Svennson, D. Buhmann, The kinetics of the reaction $CO_2 + H_2O \rightarrow H^+ + HCO_3^-$ as one of the rate limiting steps for the dissolution of calcite in the system H_2O-CO_2-$CaCO_3$, Geochim. Cosmochim. Acta, 60 (1996) 3375–3381.

[37] G.K. Batchelor, Diffusion in a field of homogeneous turbulence. II. The relative motion of particles, Math. Proc. Cambridge Philos. Soc., 48 (1952) 345–362.

[38] L.F. Richardson, Atmospheric diffusion shown on a distance/neighbor graph, Proc. R. Soc. London Ser. A, 110 (1926) 709–739.

[39] F. Jousse, T. Jongen, W. Agterof, A method to dynamically estimate the diffusion boundary layer from local velocity conditions in laminar flows, Int. J. Heat Mass Transfer, 48 (2005) 1563–1571.

[40] C.R. Blue, A. Giuffre, S. Mergelsberg, N. Han, J.J. De Yoreo, P.M. Dove, Chemical and physical controls on the transformation of amorphous calcium carbonate into crystalline $CaCO_3$ polymorphs, Geochim. Cosmochim. Acta, 196 (2017) 179–196.

[41] L.M. Hamm, A.J. Giuffre, N. Han, J. Tao, D. Wang, J.J. De Yoreo, P.M. Dove, Reconciling disparate views of template-directed nucleation through measurement of calcite nucleation kinetics and binding energies, Proc. Natl. Acad. Sci. USA, 111 (2014) 1304–1309.

[42] M. Kellermeier, A. Picker, A. Kempter, H. Cölfen, D. Gebauer, A straightforward treatment of activity in aqueous $CaCO_3$ solutions and the consequences for nucleation theory, Adv. Mater., 26 (2014) 752–757.

[43] C. Rodriguez-Navarro, K. Kudłacz, O. Cizer, E. Ruiz-Agudo, Formation of amorphous calcium carbonate and its transformation into mesostructured calcite, CrystEngComm, 17 (2015) 58–72.

[44] D. Gebauer, A. Völkel, H. Cölfen, Stable prenucleation calcium carbonate clusters, Science, 322 (2008) 1819–1822.

[45] M. Wolthers, D. Di Tommaso, Z. Du, N.H. de Leeuw, Variations in calcite growth kinetics with surface topography: molecular dynamic simulations and process-based growth kinetics modelling, CrystEngComm, 15 (2013) 5506–5514.

[46] Table of Diffusion Coefficients, Available at: http://www.aqion.de/site/194 (accessed May 28, 2019).

[47] A.A. Noyes, W.R. Whitney, The rate of solution of solid substances in their own solutions, J. Am. Chem. Soc., 19 (1897) 930–934.

[48] P. Moulin, H. Roques, Zeta potential measurement of calcium carbonate, J. Colloid Interface Sci., 261 (2003) 115–126.

[49] D. Al Mahrouqi, J. Vinogradov, M.D. Jackson, Zeta potential of artificial and natural calcite in aqueous solution, Adv. Colloid Interface Sci., 240 (2017) 60–76.

[50] R.S. Arvidsen, M. Collier, K.J. Davis, M.D. Vinson, J.E. Amonette, A. Luttge, Magnesium inhibition of calcite dissolution kinetics, Geochim. Cosmochim. Acta, 70 (2006) 583–594.

[51] R.A. Berner, The role of magnesium in the crystal growth of calcite and aragonite from sea water, Geochim. Cosmochim. Acta, 39 (1975) 489–494.

[52] M. Hänchen, V. Prigiobbe, R. Baciocchi, M. Mazzotti, Precipitation in the Mg-carbonate system-effects of temperature and CO_2 pressure, Chem. Eng. Sci., 63 (2008) 1012–1028.

[53] A. Stefansson, P. Benezeth, J. Schott, Potentiometric and spectrophotometric study of the stability of magnesium carbonate and bicarbonate ion pairs to 150°C and aqueous inorganic carbon speciation and magnesite solubility, Geochim. Cosmochim. Acta, 138 (2014) 21–31.

[54] F.C. Cadena, W.S. Midkiff, G.A. O'Connor, The calcium carbonate ion-pair as a limit to hardness removal, J. Am. Water Works Assn., 66 (1974) 524–526.

[55] J.E. Greenwood, V.W. Truesdale, A.R. Rendell, Biogenic silica dissolution in seawater - *in vitro* chemical kinetics, Prog. Oceanogr., 48 (2001) 1–23.

[56] P. Cubillas, S. Köhler, P. Manuel, C. Chaïrat, E.H. Oelkers, Experimental determination of the dissolution rates of calcite, aragonite, and bivalves, Chem. Geol., 216 (2005) 59–77.